

# Wireless Communication through Frequency Modulating Reflective Intelligent Surfaces

Jide Yuan, Elisabeth De Carvalho, and Petar Popovski

Department of Electronic Systems, Aalborg University, 9220 Aalborg, Denmark

(e-mail: {jyu,edc,petarp}@es.aau.dk)

**Abstract**—A novel frequency modulating reflecting intelligent surface (FM-RIS)-aided system has been proposed in this paper. In contrast with conventional RIS, elements over FM-RIS continuously manipulate phases of incident signals, and act as *frequency modulators* with a given frequency. Therefore, the signal received at FM-RIS is spread and transmit over a new frequency band uniquely associated to the surface, making the channels reflected from different FM-RISs separable in frequency domain. This paper studies the basic features of the proposed architecture, and demonstrates the advantages of it in terms of channel decoupling and channel estimation. The achievable spectral efficiency (SE) and the power scaling laws of FM-RIS-aided system are elaborated for large scaling systems in presence of a multiuser scenario. Simulations validate the accuracy of our analysis, and illustrate SE gain brought by FM-RIS compared with conventional mMIMO and conventional RIS-aided system.

## I. INTRODUCTION

Reconfigurable Intelligent Surface (RIS) is a meta-surface consisting of a large number of passive reflecting modules, potentially unleashing new operation modes and applications in wireless communications [1]. In most of the existing literature, the reflecting elements over the surface are assumed to be phase shifters. By intelligently adjusting the phases, RIS-aided systems are able to improve the channel propagation properties according to different communication objectives, such as higher spectrum efficiency (SE) [2], energy efficiency (EE) [3], security [4], and etc. In a typical setting, the RIS can affect some of the dominant propagation paths between a user and a Base Station (BS). The objective is that the phases of the reconfigurable elements are chosen in a way that results in maximized SNR of the received signal. To achieve this optimal passive beamforming at the RIS, it is necessary to obtain the channel state information (CSI) of both links, user-RIS and RIS-BS [2], which is difficult due to two issues. First, a RIS is passive and unable to send pilots, such that it is only possible to receive the CSI of the cascaded channel user-RIS-BS. Second, this is further complicated when the system has multiple RISs, since in this case the acquired CSI is a composite of the contributions of all RISs.

In order to overcome these two problems, we propose a new way to exploit a RIS where the RIS acts as a *frequency modulator* or mixer with a given frequency. When a signal impinges on an element of the surface, it is multiplied by a phase shifter which is time-variant and pulses at the modulator frequency. We assume for simplicity that the same frequency modulation is carried out at all the elements of the surface. When arriving at the receiver, the signals coming from the RIS can be uniquely identified by their carrier frequency shift. By

an appropriate processing, they can be separated from all the other signals that are not reflected by the RIS. In general, different parts of the RIS might operate at different frequencies. This architecture, which we term *Frequency Modulating RIS (FM-RIS)*, brings important new features. With FM-RIS, the propagation environment becomes nonlinear, as each FM operation at a RIS results in a pair of two new frequencies, not present in the transmitted signal. For example, if a receiver gets a signal through a direct path and through a FM-RIS that pulsates with a single frequency, then the received signal has three frequencies: the original one through the direct path and two resulting from the FM operation at the RIS. This means that FM-RIS increases the frequency diversity and potentially allow decoding of multiple users. Furthermore, it solves the problem of channel estimation in systems with RIS, which is challenging when the number of elements is very large. With FM-RIS, the channels from each RIS zone can be estimated in parallel, potentially leading to a large decrease in the channel acquisition overhead.

In this paper, we lay the foundation for FM-RIS communications. At this technology stage, this is a highly speculative architecture, but our objective is to investigate it from a communication-theoretic viewpoint. Conceptually, FM-RIS uses frequency mixers that are placed in the environment, rather than only at the transmitter. We outline the advantages of FM-RIS in terms of channel estimation and we elaborate on the potential gains brought by FM-RIS in terms of spectral efficiency. We start by using a simple example to introduce the basic principles behind FM-RIS and describe the details of the operation. Further on, we consider a more general FM-RIS-aided system in the uplink direction with multiple users. We investigate the feasibility of maximal-ratio combining (MRC), and zero-forcing (ZF) receivers in terms of the achievable SE. Closed form expressions for achievable SE with different receivers are derived, as well as the corresponding power scaling law. The results indicate that, benefiting from the channel decoupling feature brought by FM-RIS, the proposed FM-RIS-aided system outperforms both conventional mMIMO and conventional RIS-aided system in terms of SE.

## II. PRINCIPLE AND APPLICATION OF FM-RIS

We assume a simple model of the RIS where the incoming signal to the RIS is multiplied by a phase shift before being reflected and received by the receiver. In a conventional RIS, the phase shifts are adjusted to improve the propagation conditions according to a predefined metric. Next, we present the basic mechanism behind FM-RIS in a simple example.

### A. Basic principle

In this section, we present the principle behind FM-RIS in a simple example with single-antenna users communicating with one single-antenna BS, aided by one RIS. The goal of the RIS is to modulate the transmitted signal at a certain frequency  $f_r$ , i.e. it multiplies the incoming signal from a given user by  $\exp(2\pi f_r t)$ , where  $t$  is the time variable. Hence, the RIS creates two signals one at  $f_c + f_r$  and another one at  $f_c - f_r$  where  $f_c$  is the carrier frequency at the transmitted signal. The signal arriving via the direct path remains at the frequency  $f_c$ . Fig. 1 gives an illustration of the frequency spectrum with 4 frequency shifts over surface. We assume that all the signals and channels are narrowband. Finally, the BS isolates the signals at the different frequency bands. Hence it becomes possible to separate the signal contributions from the RIS and the signal contributions from the direct path.

This property can be exploited in different ways.

- Creation of additional degrees of freedom for user multiplexing. The modulation operation allows the creation of 2 channels and hence additional degrees of freedom. Hence, it becomes possible to multiplex 2 users. Multiple areas in the LIS can perform a modulation operation at different frequencies hence creating even more spatial degrees of freedom to support more users. In a conventional RIS system with one single-antenna BS, only one spatial degree of freedom is available.
- Channel estimation. The number of elements in a RIS is usually large so that the estimation of the channels via each element requires a long training duration. Note that estimation of each channel is necessary to adjust the phase setting in a conventional RIS system. Consider an extreme example where each of the elements of the RIS is assigned with a different frequency. We assume that the signals at the different frequencies can be separated. Hence it becomes possible to estimate each individual channel in parallel. The training duration is decreased very significantly compared to current channel estimation procedures.

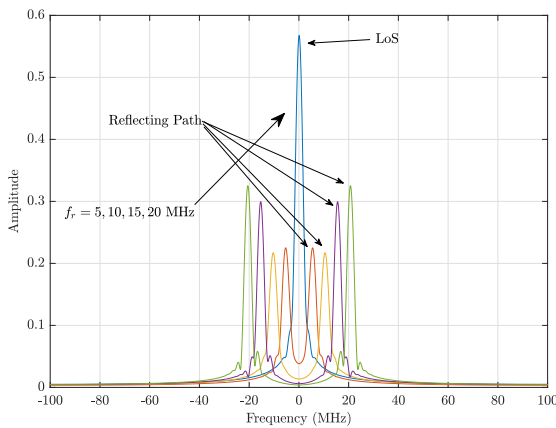


Fig. 1. An example of the frequency response of baseband signal from each path at the receiver side. The results are shown for 4 reflecting path with frequency shift  $f_r = 5, 10, 15, 20$  MHz.

### B. FM operation

Here we continue with our simple example and describe the FM operation. Each of the elements of the RIS applies the same phase shift operation:

$$\phi_r(t) = \exp(2\pi f_r t), \quad (1)$$

Denote by  $h_d(t)$ ,  $h_{us}(t)$ ,  $g_{+,sb}(t)$  and  $g_{-,sb}(t)$  the channel from the user to BS, the channel from the user to the surface, the channels from surface to BS on  $f + f_r$  and  $f - f_r$ , respectively. With a baseband signal  $x(t)$  whose frequency response is  $X(f)$  transmitted over a carrier with frequency  $f_c$ , without considering noise, the received signal at BS is described as

$$\begin{aligned} Y(f) &= H_d(f + f_c) * X(f + f_c) \\ &+ \frac{1}{2} (G_{+,sb}(f) * H_{us}(f + f_c + f_r) * X(f + f_c + f_r) \\ &+ G_{-,sb}(f) * H_{us}(f + f_c - f_r) * X(f + f_c - f_r)) \end{aligned} \quad (2)$$

in frequency domain, where  $*$  represents the convolutional product;  $H_d(f)$ ,  $H_{us}(f)$ ,  $G_{+,sb}(f)$  and  $G_{-,sb}(f)$  are the frequency response of  $h_d(t)$ ,  $h_{us}(t)$ ,  $g_{+,sb}(t)$  and  $g_{-,sb}(t)$ , respectively.

Assuming the frequency shifts  $f_r$  as known at the BS, the received signal from the frequency bands  $f_c$ ,  $f_c \pm f_r$  can thus be extracted by multiplying  $\cos(2\pi f_c t)$  and  $\cos(2\pi(f_c \pm f_r)t)$  and after a lowpass filter as:

$$\begin{cases} Y_d(f) = H_d(f_r) * X(f), \\ Y_{+,de}(f) = \frac{1}{2} (G_{+,sb}(f - f_r) * H_{us}(f) * X(f)), \\ Y_{-,de}(f) = \frac{1}{2} (G_{-,sb}(f + f_r) * H_{us}(f) * X(f)). \end{cases} \quad (3)$$

while the corresponding signals in time domain are:

$$\begin{cases} y_d(t) = h_d(t) * x(t), \\ y_{+,de}(t) = \frac{1}{2} \exp(j2\pi f_r t) h_{+,sb}(t) h_{us}(t) x(t), \\ y_{-,de}(t) = \frac{1}{2} \exp(-j2\pi f_r t) h_{-,sb}(t) h_{us}(t) x(t). \end{cases} \quad (4)$$

From (4), we separate the signals from direct paths and two replicate from the RIS. Note that  $g_{+,sb}(t)$  and  $g_{-,sb}(t)$  are mutually independent as they are the channels from  $f_c + f_r$  and  $f_c - f_r$  separately.

### C. Channel Estimation

The estimation of CSI from each individual group of FRMs can be processed in parallel benefiting from the channel decoupling. Furthermore, spreading signal over multiple frequency band allows system to accommodate more users than the BS antennas.

Followed by (4), consider two users are served in the system. Let  $\mathbf{x}_1 \in \mathbb{C}^{1 \times 2}$  and  $\mathbf{x}_2 \in \mathbb{C}^{1 \times 2}$  being the orthogonal pilots sent from user 1 and user 2 with  $\|\mathbf{x}_1\| = \|\mathbf{x}_2\| = 1$ , the received pilots at the BS can then being formulated into a matrix along with frequency domain:

$$\begin{aligned} \begin{bmatrix} \mathbf{y}_d \\ \mathbf{y}_{+,de} \\ \mathbf{y}_{-,de} \end{bmatrix} &= \frac{\sqrt{p}}{2} \mathbf{\Theta} \begin{bmatrix} h_{d,1} & h_{d,2} \\ g_{+,sb} h_{us,1} & g_{+,sb} h_{us,2} \\ g_{-,sb} h_{us,1} & g_{-,sb} h_{us,2} \end{bmatrix} \begin{bmatrix} \mathbf{x}_1 \\ \mathbf{x}_2 \end{bmatrix} + \mathbf{N} \\ &= \frac{\sqrt{p}}{2} \mathbf{\Theta} \mathbf{P} \mathbf{X} + \mathbf{N}, \end{aligned} \quad (5)$$

where  $p$  is the pilot power,  $\mathbf{\Theta}$  is a  $3 \times 3$  diagonal matrix with diagonal elements being 1,  $\exp(j2\pi f_r t)$ , and  $\exp(-j2\pi f_r t)$ ;  $h_{us,1}$  and  $h_{us,2}$  represents the channels from user 1 and user

2 to the surface, respectively;  $\mathbf{N} \in \mathbb{C}^{3 \times 2}$  is AWGN with i.i.d.  $\mathcal{CN}(0, \sigma^2)$  elements. Note that the elements in  $\mathbf{P}$  follows the “product-normal” distribution, which is symmetric around zero with unit variance. Therefore, applying the classical minimum mean square error (MMSE) estimator at BS, the cascaded channel matrix  $\mathbf{P}$  can then be detected as

$$\hat{\mathbf{P}} = \frac{2}{\sqrt{p}} [\mathbf{y}_d^T, \mathbf{y}_{+,de}^T, \mathbf{y}_{-,de}^T]^T \mathbf{X}^H \Theta^H \mathbf{D}^{-1} \quad (6)$$

where  $\mathbf{D} = \left(\sigma^2 + \frac{4}{p}\right) \mathbf{I}_k$ . Equation (6) indicates that the pilot-based channel estimation scheme is feasible in estimating the cascaded channel for user-RIS-user link, and one frequency shift over surface can double the number of connections in the system.

In a multiple FM-RISs-aided system where different frequencies uniquely associated to each FM-RIS, it is necessary to acquire the frequency shift of each surface for channel decoupling and estimation, which could be implemented by maintaining a codebook recording  $f_r, \forall r$  at BS from engineering perspective.

### III. FM-RIS-AIDED SYSTEM MODEL

In this section, we present a general system model based on which we present multiple receiver structures exploiting the additional degrees of freedom of FM-RIS. As illustrated in Fig. 2, a base station (BS) with  $M$  antennas serves  $K$  single-antenna users. A number  $N$  of FM-RISs are spread over the area enhancing the communication link between the BS and the users.

One given FM-RIS is illustrated in Fig. 3, in which frequency reconfigurable modules (FRMs) over the surface are divided into  $L$  groups each having  $S$  elements. The overall number of elements equals  $S \times L$ . Each group carries out a frequency modulation operation controlled by an oscillator. All the elements in a group are assigned the same frequency, whereas different groups are assigned different frequencies. Therefore, the signal received at surface is remodulated by FRMs to a number of different frequency band, and labelled by the frequency shift associated to the FRMs, making it possible for BS to decouple the channel by sensing the frequency shifts.

We consider a narrow band system in the uplink direction where the signals transmitted from the users are located at the same frequency band. The signal from the  $k$ th user is denoted by  $x_k(t)$ . We assume the signal received at the BS

comes from both the direct path and the reflected paths. The baseband equivalent channel of the direct path from the  $k$ th user follows a circularly-symmetric normal distribution, and is denoted as  $\mathbf{h}_{k,d}(t) \sim \mathcal{CN}(\mathbf{0}, \mathbf{I}_M)$ . Regarding the reflected paths from one FM-RIS, each path involves the channel from one user to the FM-RIS and the channel from the FM-RIS to BS. Particularly, the baseband equivalent channel from the  $k$ th user to the  $l$ th group FRMs at the  $n$ th FM-RIS is modeled as  $\mathbf{h}_{k,n_l}(t) \sim \mathcal{CN}(\mathbf{0}, \mathbf{I}_S)$ . For the FM-RIS to BS link, as we have discussed in previous section, two new frequency components appear at  $f_c \pm f_{n_l}$ , more specifically, the baseband equivalent channel from the  $l$ th group FRMs at the  $n$ th FM-RIS to the BS is then denoted by  $\mathbf{G}_{+,n_l}(t) \sim \mathcal{CN}(\mathbf{0}, \mathbf{I}_M \otimes \mathbf{I}_S)$ , and  $\mathbf{G}_{-,n_l}(t) \sim \mathcal{CN}(\mathbf{0}, \mathbf{I}_M \otimes \mathbf{I}_S)$ , where  $\otimes$  represents Kronecker product. For simplicity, we denote  $x_k(t)$ ,  $\mathbf{h}_{k,d}(t)$ ,  $\mathbf{h}_{k,n_l}(t)$ ,  $\mathbf{G}_{+,n_l}(t)$ , and  $\mathbf{G}_{-,n_l}(t)$  by  $x_k$ ,  $\mathbf{h}_{k,d}$ ,  $\mathbf{h}_{k,n_l}$ ,  $\mathbf{G}_{+,n_l}$ , and  $\mathbf{G}_{-,n_l}$ , respectively.

Note that the power of the received signal at the FM-RIS are equally distributed to  $f_c + f_{n_l}$  and  $f_c - f_{n_l}$  components as (4), hence, with equally power  $p_u$  allocated across users, the received signal at BS are the combination of following  $2NL + 1$  items:<sup>1</sup>

$$\begin{cases} \mathbf{y}_d = \sqrt{p_u} \tilde{\mathbf{H}}_d \mathbf{x} + \mathbf{n}_d, \\ \mathbf{y}_{+,n_l} = \frac{1}{2} \sqrt{p_u} \mathbf{P}_{+,n_l} \mathbf{x} + \mathbf{n}_{+,n_l}, \quad \forall n, l \\ \mathbf{y}_{-,n_l} = \frac{1}{2} \sqrt{p_u} \mathbf{P}_{-,n_l} \mathbf{x} + \mathbf{n}_{-,n_l}, \quad \forall n, l \end{cases} \quad (7)$$

where  $\tilde{\mathbf{H}}_d = [\alpha_{1,d} \mathbf{h}_{1,d}, \dots, \alpha_{K,d} \mathbf{h}_{K,d}] \in \mathbb{C}^{M \times K}$ ,  $\mathbf{x} = [x_1, \dots, x_K]^T$ ,  $\mathbf{P}_{+,n_l} = \mathbf{G}_{+,n_l} \tilde{\mathbf{H}}_{n_l}$ , and  $\mathbf{P}_{-,n_l} = \mathbf{G}_{-,n_l} \tilde{\mathbf{H}}_{n_l}$  with  $\tilde{\mathbf{H}}_{n_l} = [\alpha_{1,n_l} \mathbf{h}_{1,n_l}, \dots, \alpha_{K,n_l} \mathbf{h}_{K,n_l}] \in \mathbb{C}^{S \times K}$ .  $\mathbf{x}$  and  $\mathbf{n}$  represent the baseband signal from  $K$  users and complex Gaussian noise with  $E|\mathbf{x}|^2 = 1$  and  $\mathbf{n} \sim \mathcal{CN}(\mathbf{0}, \mathbf{I}_M \sigma^2)$  ( $\sigma^2$  is AWGN power), respectively;  $\alpha_{k,d}$  and  $\alpha_{k,n_l}$  are the channel gain for direct path and reflecting path from the  $l$ th group on the  $n$ th surface of the  $k$ th user.

As the signals are separable in the frequency domain, we are able to pack the signals from all frequency bands into a vector as

$$\mathbf{y}_{\text{all}} = \sqrt{p_u} \mathbf{H}_{\text{all}} \mathbf{x} + \mathbf{n}_{\text{all}}, \quad (8)$$

<sup>1</sup>In practice, there are signal components that are not reflecting from the FM-RISs. We ignore these components in following analysis, and leave the analysis that includes them to future work.

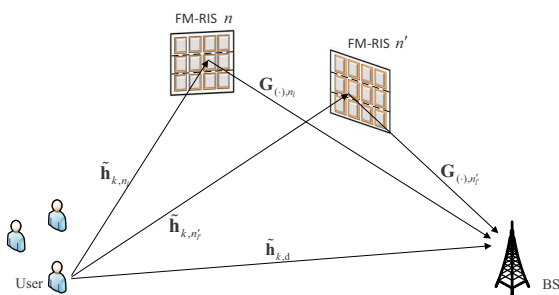


Fig. 2. The diagram illustrates the FM-RIS-aided communication systems, where  $K$  single antenna users are served by BS with  $N$  FM-RIS assisting the connections.

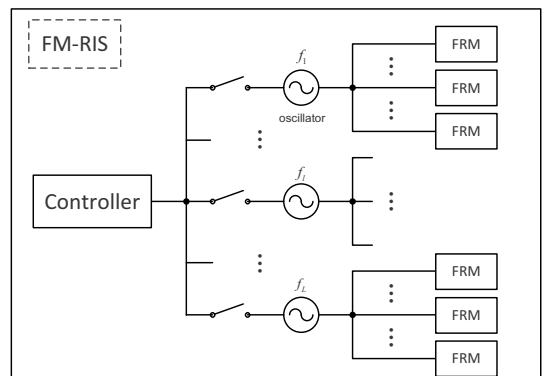


Fig. 3. A FM-RIS structure where FRMs are divided into multiple groups, and FRMs in one groups associate to a particular oscillator with fixed frequency  $f_i$ .

$$\text{SINR}_{\text{MRC}} = \frac{\alpha_{k,d}^2 \left( M^2 \alpha_{k,d}^2 + \frac{1}{2} M^3 \eta \sum_{n,l} \alpha_{k,n_l}^2 \right) + \frac{1}{8} M^4 \eta^2 \left( \sum_{n,l} \alpha_{k,n_l}^4 + \sum_{n,l} \alpha_{k,n_l}^2 \sum_{n',l' \neq n,l} \alpha_{k,n'l'}^2 \right)}{M \alpha_{k,d}^2 \alpha_{k',d}^2 + \frac{1}{8} M^3 \eta \sum_{n,l} \alpha_{k,n_l}^2 \sum_{k' \neq k} \alpha_{k',n_l}^2 + \frac{1}{\rho_u} \left( M \alpha_{k,d}^2 + M^2 \eta \sum_{n=1}^N \sum_{l=1}^L \alpha_{k,n_l}^2 \right)} \quad (15)$$

where

$$\mathbf{y}_{\text{all}} = [\mathbf{y}_d^T, \mathbf{y}_{+,1_1}^T, \dots, \mathbf{y}_{+,N_L}^T, \mathbf{y}_{-,1_1}^T, \dots, \mathbf{y}_{-,N_L}^T]^T \quad (9)$$

$$\mathbf{H}_{\text{all}} = \left[ \tilde{\mathbf{H}}_d^T, \frac{1}{2} \mathbf{P}_{+,1_1}^T, \dots, \frac{1}{2} \mathbf{P}_{+,N_L}^T, \frac{1}{2} \mathbf{P}_{-,1_1}^T, \dots, \frac{1}{2} \mathbf{P}_{-,N_L}^T \right]^T \quad (10)$$

$$\mathbf{n}_{\text{all}} = [\mathbf{n}_d^T, \mathbf{n}_{+,1_1}^T, \dots, \mathbf{n}_{+,N_L}^T, \mathbf{n}_{-,1_1}^T, \dots, \mathbf{n}_{-,N_L}^T]^T \quad (11)$$

Denoting by  $\mathbf{W} \in \mathbb{C}^{(2MNL+1) \times K}$  the receivers for the all channels. The achievable SE of the  $k$ th user then equals to

$$R_k = \log_2(1 + \text{SINR}_k), \quad (12)$$

where

$$\text{SINR}_k = \frac{\|\mathbf{w}_k^H \mathbf{h}_{k,\text{all}}\|^2}{\sum_{k' \neq k} \|\mathbf{w}_k^H \mathbf{h}_{k',\text{all}}\|^2 + \frac{1}{\rho_u} \|\mathbf{w}_k^H\|^2}, \quad (13)$$

where  $\rho_u = \frac{p_u}{\sigma^2}$ ,  $\mathbf{w}_k$  and  $\mathbf{h}_{k,\text{all}}$  are the  $k$ th column of  $\mathbf{W}$  and  $\mathbf{H}_{\text{all}}$ , respectively.

#### IV. ASYMPTOTIC ANALYSIS OF LARGE-SCALE FM-RIS-AIDED SYSTEM

In this section, we provide asymptotic results for the achievable SINR with different receivers. The following assumption is made in this section for theoretical analysis.

*Assumption 1:* We assume a fixed ratio  $\eta$  between the number of antennas at BS and the number of FRMs in a group, i.e.,  $\eta = S/M$  with  $0 < \eta < 1$ .

We consider the CSI is known at the BS,<sup>2</sup> and two conventional linear receivers MRC and ZF are applied at BS, i.e.,

$$\mathbf{W} = \begin{cases} \mathbf{H}_{\text{all}}, & \text{MRC,} \\ \mathbf{H}_{\text{all}} (\mathbf{H}_{\text{all}}^H \mathbf{H}_{\text{all}})^{-1}, & \text{ZF.} \end{cases} \quad (14)$$

##### A. MRC

When MRC is applied at the BS, i.e.,  $\mathbf{W}^H = \mathbf{H}_{\text{all}}^H$ , we can obtain the achievable rate at the BS for the  $k$ th user.

*Proposition 1:* The achievable SINR at the BS for the  $k$ th user with MRC is given in (15) at the top of next page. Assume that the transmit power of user is scaled with  $M^2$ , i.e.,  $\rho_u = \frac{E_u}{M^2}$  with fixed  $E_u$ , the SINR converges to

$$\text{SINR}_{\text{MRC}} \xrightarrow[M \rightarrow \infty]{a.s.} \frac{1}{8} E_u \eta \frac{\sum_{n,l} \alpha_{k,n_l}^4 + \sum_{n,l} \alpha_{k,n_l}^2 \sum_{n',l' \neq n,l} \alpha_{k,n'l'}^2}{\sum_{n=1}^N \sum_{l=1}^L \alpha_{k,n_l}^2} \quad (16)$$

with  $M \rightarrow \infty$ .

*Proof:* See Appendix A.  $\blacksquare$

Note that the power scaling law of achievable SINR with MRC receiver is different from conventional mMIMO system,

<sup>2</sup>System performance with imperfect CSI is interesting for additional research, we do not pursue it herein due to space constraints.

i.e.,  $\rho_u = \frac{E_u}{M^2}$  instead of  $\rho_u = \frac{E_u}{M}$ . This observation illustrates that even the transmit power of each user is scaled down with  $M$ , the achievable SINR will grow without bound. This is due to the fact that the signal received at a surface is diversified to  $2SL$  streams in frequency domain, and therefore creates  $2MSL$  new channels for each signal. It allows the transmit power to scale down by  $2MSL$  to maintain the achievable performance. Along with  $\eta = S/M$  in our case, FM-RIS-aided system can hence provide services with much less power compared with conventional mMIMO.

##### B. ZF

With ZF,  $\mathbf{W}^H \mathbf{H}_{\text{all}} = \mathbf{I}_K$ . In other words, we have

$$\mathbf{w}_{i,d}^H \mathbf{h}_{j,\text{all}} = \begin{cases} 1, & i=j, \\ 0, & i \neq j. \end{cases} \quad (17)$$

From (13), the achievable SINR for the  $k$ th user is then given the following proposition.

*Proposition 2:* The achievable SINR at the BS for the  $k$ th user with ZF receiver is lower bounded by

$$\text{SINR}_{\text{ZF}} = \rho_u \left( M \alpha_{k,d}^2 + \frac{1}{2} M^2 \eta \sum_{n=1}^N \sum_{l=1}^L \alpha_{k,n_l}^2 \right). \quad (18)$$

Assume that the transmit power of user is scaled with  $M^2$ , i.e.,  $\rho_u = \frac{E_u}{M^2}$  with fixed  $E_u$ , If  $M \rightarrow \infty$  with fixed  $\eta$ ,  $\text{SINR}_{\text{ZF}}$  converges to

$$\text{SINR}_{\text{ZF}} \xrightarrow[M \rightarrow \infty]{a.s.} \frac{1}{2} \eta E_u \sum_{n=1}^N \sum_{l=1}^L \alpha_{k,n_l}^2. \quad (19)$$

*Proof:* See Appendix B.  $\blacksquare$

*Corollary 1:* When  $M \rightarrow \infty$  with fixed  $S$ , (18) converges to

$$\text{SINR}_{\text{ZF}} \xrightarrow[M \rightarrow \infty]{a.s.} E_u \left( \alpha_{k,d}^2 + \frac{S}{2} \sum_{n=1}^N \sum_{l=1}^L \alpha_{k,n_l}^2 \right) \quad (20)$$

with the transmit power being scaled with  $M$ .

Same power scaling law of achievable SINR can be observed for ZF receiver as well. Equation (19) further indicates that the achievable SINR grows linearly with the number of FM-RISs and the number of groups in a FM-RIS, where the noise power from direct path can be ignored compared with that introduced by FM-RISs. *Corollary 1* illustrates the case where limited number of FRMs deployed on FM-RISs. From (20), we note that the power scaling law becomes  $\rho_u = E_u/M$  as conventional mMIMO, but more power can be detected from reflecting paths which enhances the performance.

It is worth noting that the separate knowledge of  $\mathbf{G}_{(\cdot),n_l}$  and  $\mathbf{H}_{n_l}$  is not required for *Proposition 1-2* to be valid, while only the cascaded channel  $\mathbf{P}_{(\cdot),n_l}$  is enough. This largely reduces the workload of channel estimation in which the

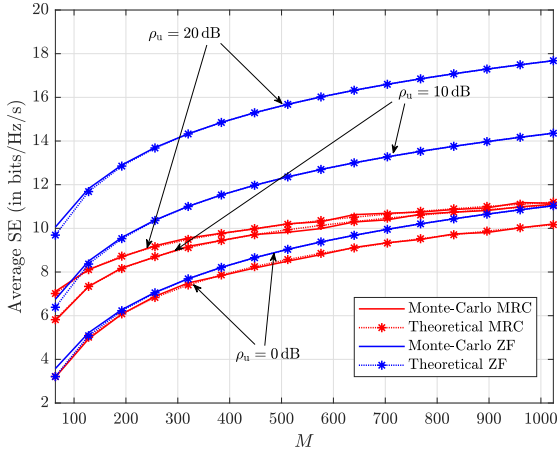


Fig. 4. The analytical and numerical results of SE for MRC and ZF with different numbers of BS antennas. The results are shown for  $N = 4$ ,  $L = 4$ , and  $K = 10$ .

separate estimation of  $\mathbf{G}_{(\cdot),n_i}$  and  $\mathbf{H}_{n_i}$  is a challenging task for conventional RIS-aided system.

## V. NUMERICAL RESULTS

In our simulations, the BS is deployed at the center of a  $1 \text{ km}^2$  area, while  $N$  FM-RISs and  $K$  users are randomly distributed in the area. The ratio  $\eta$  is set to  $1/4$ . For the channel gains which consist of path directs and shadowing, we adopt the model in [5], and is given as (in dB)

$$\alpha = 32.9 + 36.3 \log_{10} d, \quad (21)$$

where  $d$  (in m) represents the overall distance between two antennas.

We first validate the accuracy of our analytical results in Fig. 4. Fig. 4 compares the numerical results of the achievable SE with proposed analytical results for MRC and ZF receivers with different transmit power. Clearly, it can be observed that the proposed results match the numerical SE very tight, especially at large  $M$ . Moreover, it is rather effective for ZF to improve the performance by increasing transmit power, e.g., 6 bits/Hz/s gain for ZF by improving  $\rho_u$  from 0 dB to 20 dB with  $M = 400$  while only 2 bits/Hz/s for MRC.

Fig. 5 compares the achievable SE for FM-RIS-aided system and conventional RIS-aided system for MRC and ZF receivers. In the simulation, every phase shifters on conventional RISs are set to 1, which is fair since without channel decoupling, CSI of each path is inaccessible making the shift optimization over RIS infeasible. We can observe FM-RIS-aided system outperforms conventional RIS-aided system for both MRC and ZF receivers, which is benefited from the channel decoupling.

Finally, we illustrate the power scaling laws. Fig. 6 shows the spectral efficiency for FM-RIS-aided system with MRC and ZF receivers. With  $\rho_u = E_u/M$  and with increasing  $M$ , the achievable SE converges to a constant value for conventional mMIMO with both receivers while growing logarithmically without bound for FM-RIS-aided system, as expected. Instead, if  $\rho_u = E_u/M^2$ , SE converges to a non-zero value for FM-RIS-aided system with both receivers, while converging to zero for conventional mMIMO. The results

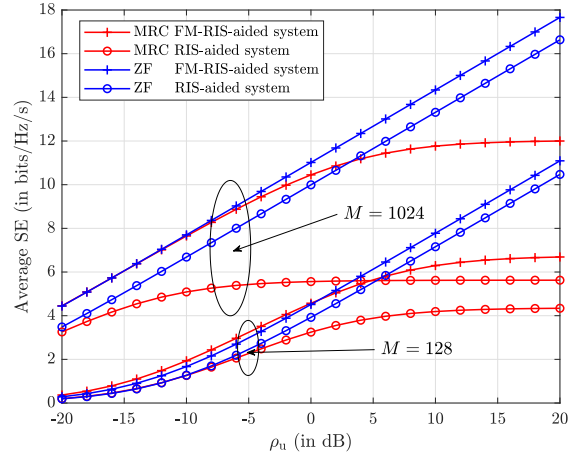


Fig. 5. The comparison of SE for FM-RIS-aided system and conventional RIS-aided system with MRC and ZF receivers. The results are shown for  $N = 4$ ,  $L = 4$ , and  $K = 10$ .

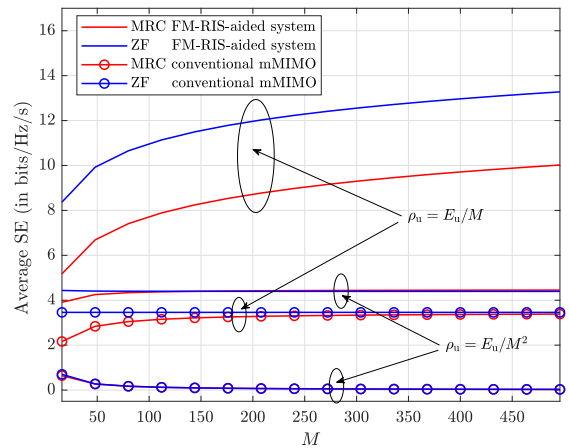


Fig. 6. The comparison of power scaling law for FM-RIS-aided system and conventional mMIMO with MRC and ZF receivers. The reference transmit power is  $E_u = 10 \text{ dB}$ . The results are shown for  $N = 4$ ,  $L = 4$ , and  $K = 10$ .

validate our theoretical analysis that the transmit power of each user can be scaled down by  $M^2$  for FM-RIS-aided system.

## VI. CONCLUSION

In the paper, we proposed a novel FM-RIS-aided system, where FM-RIS consists of a number of modules that are capable of manipulating frequency of the incident signals. We first investigated the basic principles of FM-RIS architecture, and illustrated the advantages of it in terms of channel decoupling. Then, the closed forms of asymptotic SE with MRC and ZF receivers were evaluated for large scaling systems in presence of a multiuser scenario. The results showcased a different power scaling law of FM-RIS-aided system compared with conventional mMIMO, indicating the transmit power can be further scaled down in FM-RIS-aided system. The simulations verified our theoretical results, and demonstrated that the proposed FM-RIS-aided system outperforms conventional mMIMO and conventional RIS-aided system in terms of SE due to the channel decoupling feature brought by FM-RIS.

APPENDIX A  
PROOF OF PROPOSITION 1

It is clearly that  $\mathbf{w}_k^H \mathbf{h}_{k,\text{all}} = \mathbf{h}_{k,\text{all}}^H$ , where

$$\mathbf{h}_{k,\text{all}} = \left[ \tilde{\mathbf{h}}_{k,d}^T, \frac{1}{2} \mathbf{p}_{k,+}^T, \dots, \frac{1}{2} \mathbf{p}_{k,+}^T, \frac{1}{2} \mathbf{p}_{k,-}^T, \dots, \frac{1}{2} \mathbf{p}_{k,-}^T \right]^T \quad (22)$$

with  $\tilde{\mathbf{h}}_{k,d}^T$ ,  $\mathbf{p}_{k,+}^T$  and  $\mathbf{p}_{k,-}^T$  being the  $k$ th column of  $\tilde{\mathbf{H}}_d^T$ ,  $\mathbf{P}_{+,n_l}^T$  and  $\mathbf{P}_{-,n_l}^T$ , respectively. Then, the effective channel of  $k$ th user can be evaluated as

$$\begin{aligned} \mathbf{w}_k^H \mathbf{h}_{k,\text{all}} &= \tilde{\mathbf{h}}_{k,d}^H \tilde{\mathbf{h}}_{k,d} \\ &+ \frac{1}{4} \sum_{n=1}^N \sum_{l=1}^L (\mathbf{p}_{k,+}^H \mathbf{p}_{k,+} + \mathbf{p}_{k,-}^H \mathbf{p}_{k,-}). \end{aligned} \quad (23)$$

Utilizing the result of large random theory, we have following deterministic equivalent for direct path:

$$\frac{1}{M} \tilde{\mathbf{h}}_{k,d}^H \tilde{\mathbf{h}}_{k,d} \xrightarrow[M \rightarrow \infty]{a.s.} \alpha_{k,d}^2, \quad (24)$$

$$\frac{1}{M^2} \left( \tilde{\mathbf{h}}_{k,d}^H \tilde{\mathbf{h}}_{k,d} \right)^2 \xrightarrow[M \rightarrow \infty]{a.s.} \alpha_{k,d}^4, \quad (25)$$

$$\frac{1}{M} \tilde{\mathbf{h}}_{k,d}^H \tilde{\mathbf{h}}_{k',d} \xrightarrow[M \rightarrow \infty]{a.s.} 0, \quad (26)$$

$$\frac{1}{M} \left( \tilde{\mathbf{h}}_{k,d}^H \tilde{\mathbf{h}}_{k',d} \right)^2 \xrightarrow[M \rightarrow \infty]{a.s.} \alpha_{k,d}^2 \alpha_{k',d}^2. \quad (27)$$

To evaluate the items from reflecting paths, we first notice that  $\mathbf{R}_{+,n_l} = \mathbf{G}_{+,n_l}^H \mathbf{G}_{+,n_l}$  is a typical central Wishart matrix, and the expectation of its unordered eigenvalue  $\lambda$  equals to the larger dimension of matrix  $\mathbf{G}_{+,n_l}$ , i.e.,  $E[\lambda] = M$ . Along with the result that  $\frac{1}{MS} \text{tr} \mathbf{R}_{+,n_l} \xrightarrow[M \rightarrow \infty]{a.s.} \frac{1}{M} E[\lambda] = 1$ , and recalling  $S = M\eta$ , we can observe following results [6, Lemma 4]:

$$\frac{1}{M^2 \eta} \mathbf{p}_{k,+}^H \mathbf{p}_{k,+} \xrightarrow[M \rightarrow \infty]{a.s.} \frac{\alpha_{k,n_l}^2}{M^2 \eta} \text{tr} \mathbf{R}_{+,n_l} = \alpha_{k,n_l}^2, \quad (28)$$

$$\frac{1}{M^4 \eta^2} \left( \mathbf{p}_{k,+}^H \mathbf{p}_{k,+} \right)^2 \xrightarrow[M \rightarrow \infty]{a.s.} \alpha_{k,n_l}^4, \quad (29)$$

$$\frac{1}{M^2 \eta} \mathbf{p}_{k,+}^H \mathbf{p}_{k',+} \xrightarrow[M \rightarrow \infty]{a.s.} 0, \quad (30)$$

$$\frac{1}{M^3 \eta} \left( \mathbf{p}_{k,+}^H \mathbf{p}_{k',+} \right)^2 \xrightarrow[M \rightarrow \infty]{a.s.} \alpha_{k,n_l}^2 \alpha_{k',n_l}^2. \quad (31)$$

As the signal power are equally shared in frequency  $f_c \pm f_{n_l}$ , we can obtain same deterministic equivalents as (28)-(31) for channel  $\mathbf{p}_{k,-,n_l}$ .

With the results of (24)-(25) and (28)-(29), we can evaluate the power of effective channel as

$$\begin{aligned} \|\mathbf{w}_k^H \mathbf{h}_{k,\text{all}}\|^2 &\xrightarrow[M \rightarrow \infty]{a.s.} \alpha_{k,d}^2 \left( M^2 \alpha_{k,d}^2 + \frac{1}{2} M^3 \eta \sum_{n,l} \alpha_{k,n_l}^2 \right) \\ &+ \frac{1}{8} M^4 \eta^2 \left( \sum_{n,l} \alpha_{k,n_l}^4 + \sum_{n,l} \alpha_{k,n_l}^2 \sum_{n' \neq n \text{ or } l' \neq l} \alpha_{k,n'l'}^2 \right). \end{aligned} \quad (32)$$

The interference from the  $k'$ th user can be evaluated as

$$\begin{aligned} \mathbf{w}_k^H \mathbf{h}_{k',\text{all}} &= \tilde{\mathbf{h}}_{k,d}^H \tilde{\mathbf{h}}_{k',d} \\ &+ \frac{1}{4} \sum_{n=1}^N \sum_{l=1}^L (\mathbf{p}_{k,+}^H \mathbf{p}_{k',+} + \mathbf{p}_{k,-}^H \mathbf{p}_{k',-}). \end{aligned} \quad (33)$$

With the the results of (26)-(27) and (30)-(31), we yield that

$$\|\mathbf{w}_k^H \mathbf{h}_{k',\text{all}}\|^2 \xrightarrow[M \rightarrow \infty]{a.s.} M \alpha_{k,d}^2 \alpha_{k',d}^2 + \frac{1}{8} M^3 \eta \sum_{n,l} \alpha_{k,n_l}^2 \alpha_{k',n_l}^2. \quad (34)$$

Similarly, the noise power can be evaluated in the same way, and is given as

$$\|\mathbf{w}_k\|^2 \xrightarrow[M \rightarrow \infty]{a.s.} M \alpha_{k,d}^2 + \frac{M^2 \eta}{2} \sum_{n=1}^N \sum_{l=1}^L \alpha_{k,n_l}^2. \quad (35)$$

Substituting (32), (34) and (35) into (13) and after some manipulations, we complete the proof.

APPENDIX B  
PROOF OF PROPOSITION 2

Substituting (17) into (13), we can obtain the achievable SINR using similar methodology in [7] as

$$\text{SINR}_{\text{ZF}} = \frac{1}{\frac{1}{\rho_u} \left( \left[ \left( \mathbf{H}_{k,\text{all}}^H \mathbf{H}_{k,\text{all}} \right)^{-1} \right]_{kk} \right)} \quad (36)$$

where  $[\cdot]_{kk}$  represents the  $(k, k)$ th element of matrix.

Again, with the same methods used in (24)-(31), we observe that the matrix  $\mathbf{H}_{k,\text{all}}^H \mathbf{H}_{k,\text{all}}$  converges to a deterministic matrix whose  $(i, j)$ th element is given as

$$\begin{aligned} \left\{ \mathbf{H}_{k,\text{all}}^H \mathbf{H}_{k,\text{all}} \right\}_{ij} &\xrightarrow[M \rightarrow \infty]{a.s.} \begin{cases} M \alpha_{k,d}^2 + \frac{M^2 \eta}{2} \sum_{n=1}^N \sum_{l=1}^L \alpha_{k,n_l}^2, & i = j, \\ 0, & i \neq j. \end{cases} \end{aligned} \quad (37)$$

Therefore, we clearly yield

$$\begin{aligned} \left[ \left( \mathbf{H}_{k,\text{all}}^H \mathbf{H}_{k,\text{all}} \right)^{-1} \right]_{kk} &\xrightarrow[M \rightarrow \infty]{a.s.} \left( M \alpha_{k,d}^2 + \frac{1}{2} M^2 \eta \sum_{n=1}^N \sum_{l=1}^L \alpha_{k,n_l}^2 \right)^{-1}. \end{aligned} \quad (38)$$

Substituting (38) into (36) along with the fact  $\rho_u = \frac{E_u}{M^2}$ , we complete the proof.

REFERENCES

- [1] E. Basar, "Reconfigurable intelligent surface-based index modulation: A new beyond MIMO paradigm for 6G," *IEEE Trans. Commun.*, pp. 1–1, Feb. 2020.
- [2] Y. Yang, B. Zheng, S. Zhang, and R. Zhang, "Intelligent reflecting surface meets OFDM: Protocol design and rate maximization," *IEEE Trans. Commun.*, pp. 1–1, Mar. 2020.
- [3] C. Huang, A. Zappone, G. C. Alexandropoulos, M. Debbah, and C. Yuen, "Reconfigurable intelligent surfaces for energy efficiency in wireless communication," *IEEE Trans. Wireless Commun.*, vol. 18, no. 8, pp. 4157–4170, 2019.
- [4] M. Cui, G. Zhang, and R. Zhang, "Secure wireless communication via intelligent reflecting surface," *IEEE Wireless Commun. Lett.*, vol. 8, no. 5, pp. 1410–1414, 2019.
- [5] J. Hoydis, K. Hosseini, S. Ten Brink, and M. Debbah, "Making smart use of excess antennas: Massive MIMO, small cells, and TDD," *Bell Labs Technical Journal*, vol. 18, no. 2, pp. 5–21, Sep. 2013.
- [6] J. Hoydis and S. ten Brink, and M. Debbah, "Massive MIMO in the UL/DL of cellular networks: How many antennas do we need?" *IEEE J. Sel. Areas Commun.*, vol. 31, no. 2, pp. 160–171, Feb. 2013.
- [7] H. Q. Ngo, E. G. Larsson, and T. L. Marzetta, "Energy and spectral efficiency of very large multiuser MIMO systems," *IEEE Trans. Commun.*, vol. 61, no. 4, pp. 1436–1449, Apr. 2013.